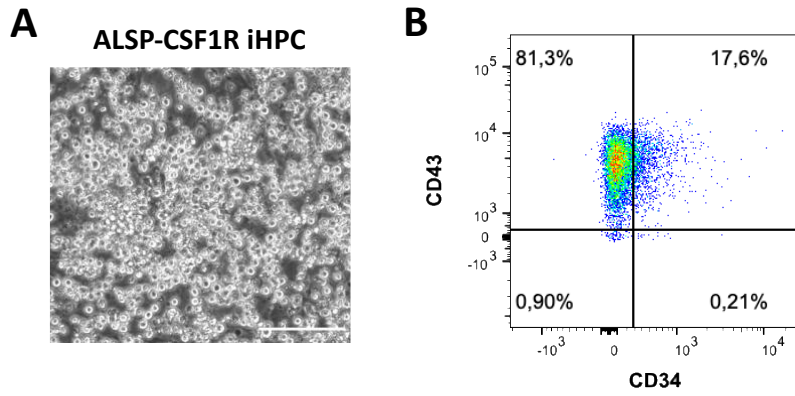
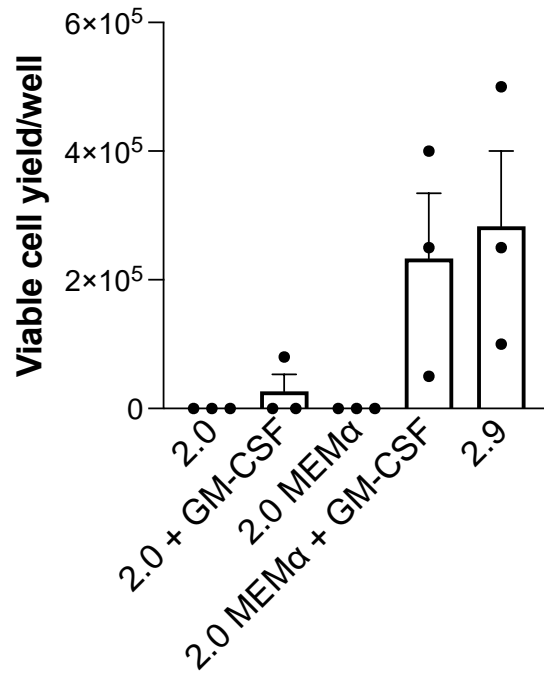


**Figure S18. Quality control of the ALSP-CSF1R iPSC line.** (A) Immunostaining of pluripotency markers. (B) Chromatogram of the heterozygous c.2350G>A variant in the *CSF1R* gene (shown here at position 150). (C) G-band assay showing normal karyotype of ALSP-CSF1R iPSCs. (D) qPCR-based assessment of copy numbers of chromosomal regions prone to karyotypic abnormalities.



**Figure S19. iHPCs generated from ALSP-CSF1R iPSCs.** (A) Phase contrast image of iHPC culture on day 12 of differentiation (scale bar = 150  $\mu\text{m}$ ). (B) Flow cytometry assessment of CD43 and CD34 in iHPCs on day 12 of differentiation.



**Figure S20. Cell yield following microglial differentiation of ALSP-CSF1R iHPCs using various media formulations.** Viable cell yield per well of a 6-well plate assessed by trypan blue exclusion assay. n = 3 differentiation batches.

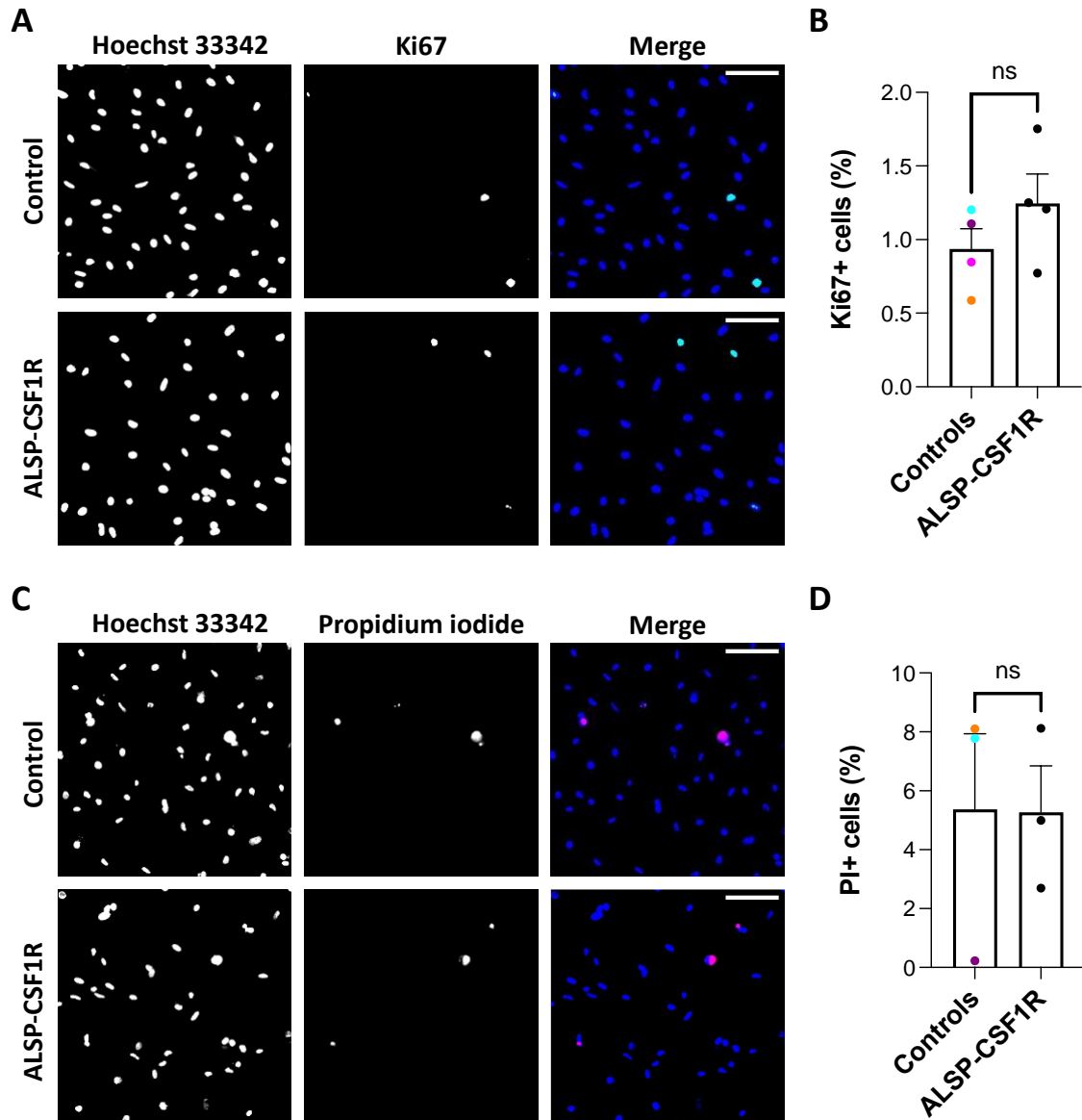


**Figure S21. Assessment of proliferation and death rate in mature ALSP-CSF1R iMGL culture.** (A) Representative images of Ki67 immunostaining. Scale bar = 50  $\mu$ m. (B) Quantification of Ki67-immunopositivity. A t-test was performed. n = 3 healthy control lines and 3 batches of a single ALSP patient line, differentiated side-by-side, ns = non-significant. (C) Representative images of propidium iodide staining. Scale bar = 50  $\mu$ m. (D) Quantification of propidium iodide (PI) -positivity. A t-test was performed. n = 3 healthy control lines and 3 batches of a single ALSP patient line, differentiated side-by-side, ns = non-significant.

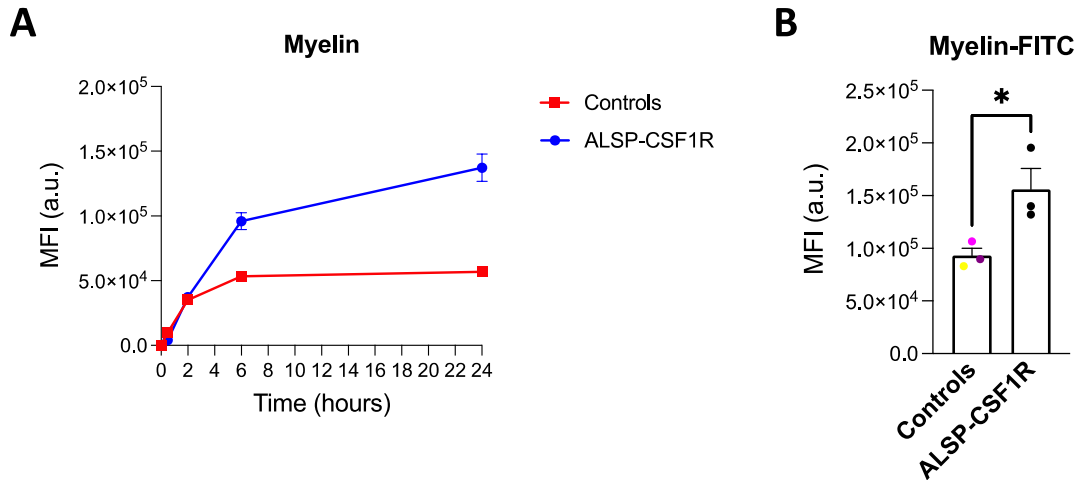


**Figure S22. Myelin uptake by ALSP-CSF1R iMGL.** iMGL 2.9 were exposed to pHrodo Green<sup>TM</sup> (A) or FITC (B) -labelled myelin. Cells were counterstained with Hoechst 33342 and mean green fluorescence intensity (MFI) was measured (a.u. = arbitrary unit). (A) Mean +/- standard deviation of three technical replicates are presented. n = 1 healthy control line and 1 batch of an ALSP patient line, differentiated side-by-side. (B) Cells were exposed for three hours. A t-test was performed. n = 3 healthy control lines and 3 batches of a single ALSP patient line, differentiated side-by-side, \* p < 0.05.

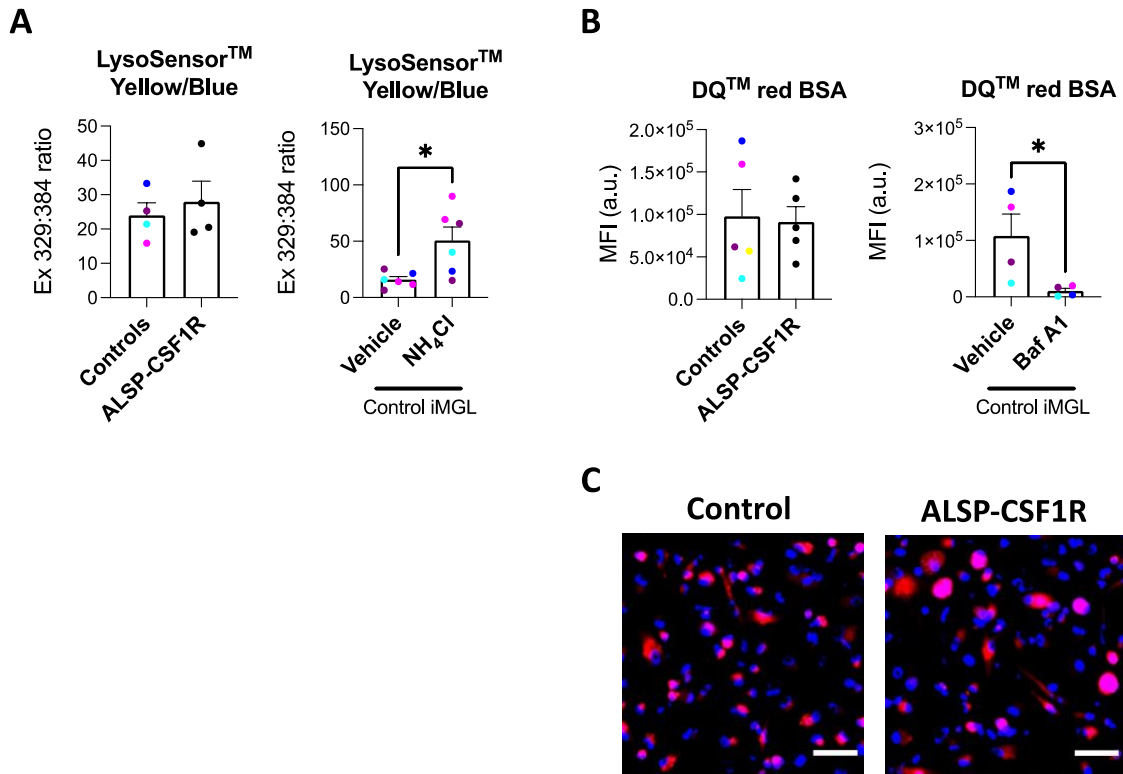


**Figure S23. Lysosomal function of ALSP-CSF1R iMGL.** All iMGL were generated using the 2.9 protocol. (A) Assessment of lysosomal pH using LysoSensor™ Yellow/Blue. Cell treatment with 50 mM ammonium chloride (NH<sub>4</sub>Cl) was used as a positive control. Left panel: n = 4 healthy control lines and 4 batches of a single ALSP patient line, differentiated side-by-side. Right panel: n = 6 batches from 4 healthy control lines. T-tests were performed, \* p < 0.05. (B-C) Assessment of lysosomal protease activity using DQ™ red BSA. (B) Cell treatment with bafilomycin A1 (Baf A1, 100 nM) was used as a control. MFI = mean fluorescence intensity, a.u. = arbitrary unit. Left panel: n = 5 healthy control lines and 5 batches of a single ALSP patient line, differentiated side-by-side. Right panel: T-tests were performed. n = 4 healthy control lines, \* p < 0.05. (C) Representative fluorescence images. Scale bar = 50 μm.

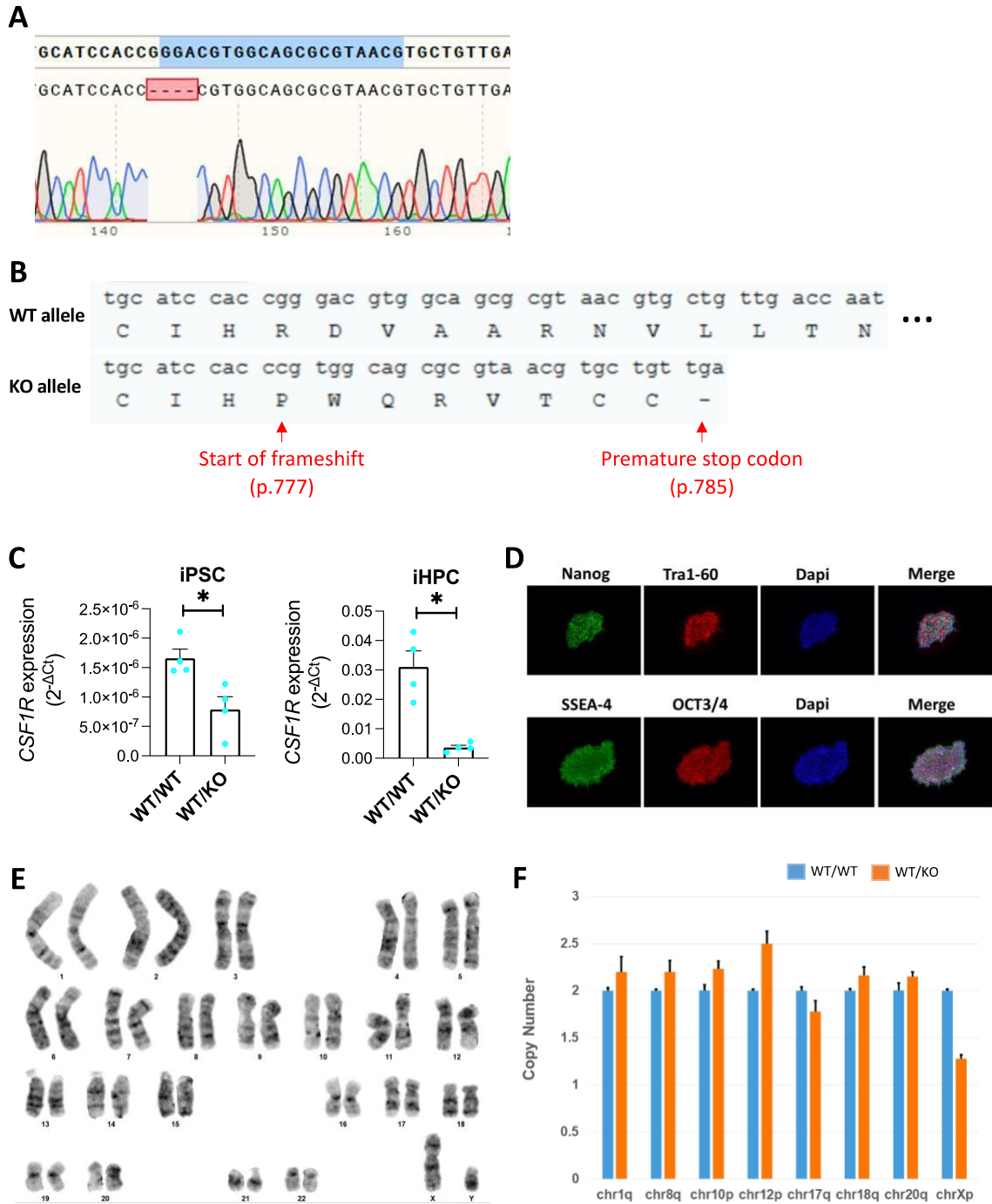


**Figure S24. Quality control of the *CSF1R*<sup>WT/KO</sup> iPSC line.** (A) Chromatogram of the heterozygous 4-base pair deletion (c.2330\_2333del) in *CSF1R*. Shaded area of the sequence represents the position recognized by the guide RNA. (B) Protein sequence predicted using ExPASy Translate tool (<https://web.expasy.org/translate/>). (C) qRT-PCR

assessment of *CSF1R* expression in iPSCs and iHPCs. Mann-Whitney tests were performed. n = 4 differentiation batches, \* p < 0.05. *CSF1R*<sup>WT/WT</sup> and *CSF1R*<sup>WT/KO</sup> cells were differentiated side-by-side into iHPCs. (D) Immunostaining of pluripotency markers in iPSCs. (E) G-band assay showing normal karyotype of ALSP-*CSF1R* iPSCs. (F) qPCR-based assessment of copy numbers of chromosomal regions prone to karyotypic abnormalities in iPSCs.



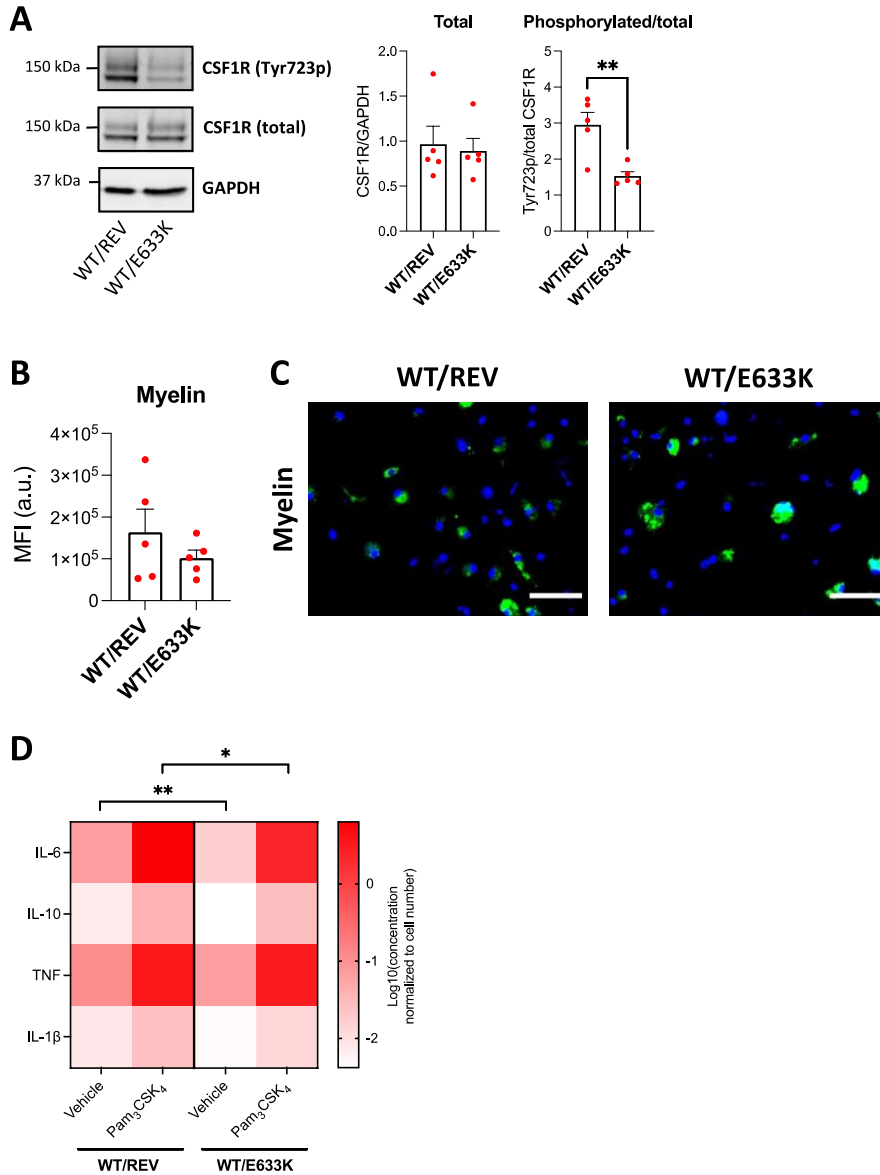


**Figure S25. Functional features of  $CSF1R^{WT/E633K}$  iMGL compared to their isogenic controls.**  $CSF1R^{WT/REV}$  and  $CSF1R^{WT/E633K}$  iPSCs were differentiated into iMGL side-by-side using the 2.9 protocol. (A) Western blot assessment of CSF1R and its tyrosine 723-phosphorylated form, and GAPDH. A t-test was performed.  $n = 5$  differentiation batches,  $** p < 0.01$ . (B-C) iMGL were exposed for three hours to pHrodo™ Green-labelled myelin debris. Cells were counterstained with Hoechst 33342 and mean green fluorescence intensity (MFI) was measured (a.u. = arbitrary unit). (B) Quantification of MFI. A t-test was performed.  $n = 5$  differentiation batches. (C) Representative fluorescence images. Scale bar = 50  $\mu\text{m}$ . (D) Cytokine concentrations measured in cell supernatants following a

24-hour treatment with vehicle or Pam<sub>3</sub>CSK<sub>4</sub> (100 ng/mL). Two-way ANOVA were performed, followed by Tukey's post hoc test. n = 5 differentiation batches, \* p < 0.05, \*\* p < 0.01.

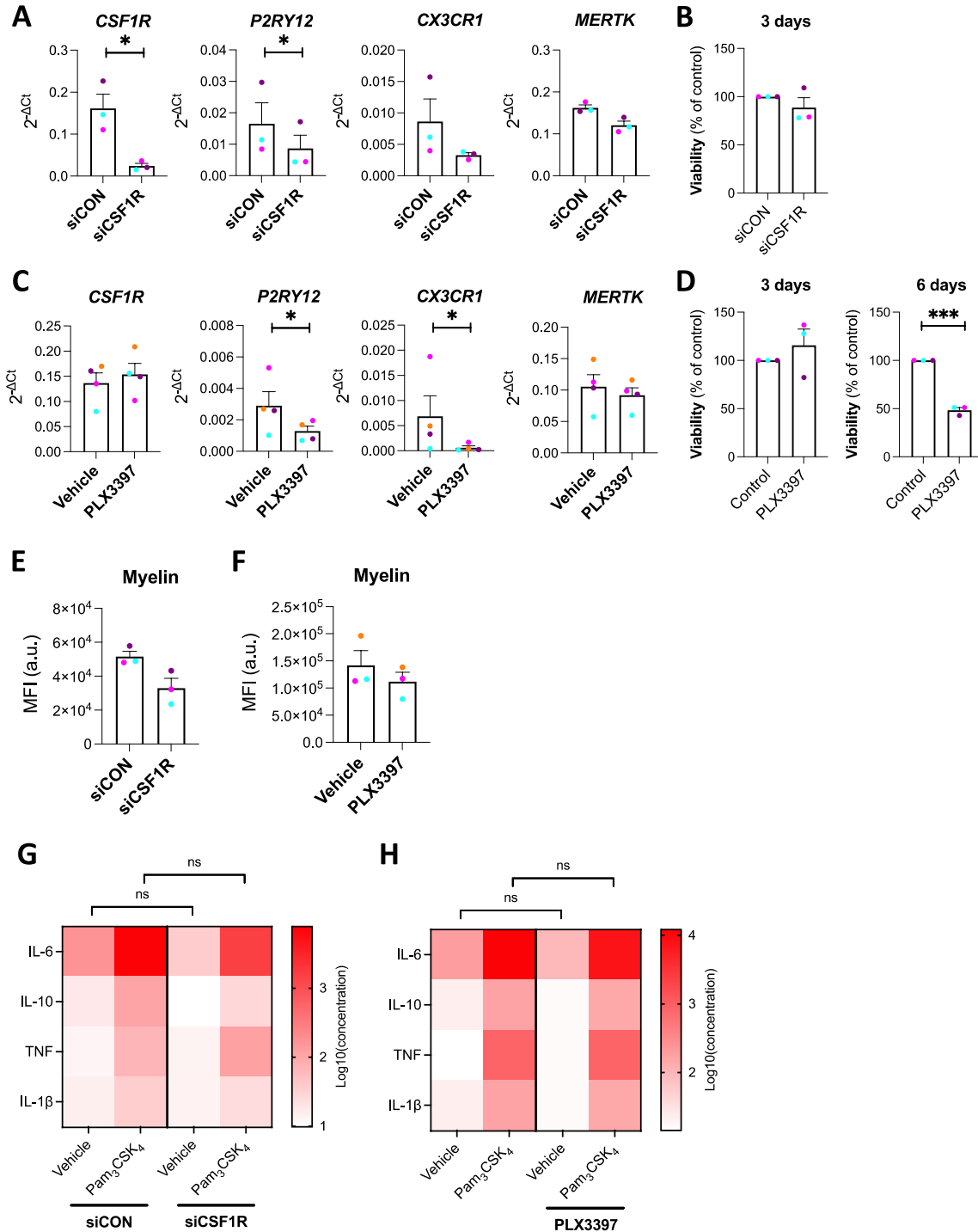


**Figure S26. Effect of CSF1R knockdown or inhibition on mature iMGL.** Healthy control, mature iMGL were generated following the 2.9 protocol. (A) Microglia marker expression assessed by qRT-PCR in iMGL three days after siCON or siCSF1R transfection.

T-tests were performed.  $n = 3$  lines, \*  $p < 0.05$ . (B) Viability of iMGL three days after siCON or siCSF1R transfection. A Mann-Whitney test was performed.  $n = 3$  lines. (C) Microglia marker expression assessed by qRT-PCR in iMGL following a 3-day treatment with PLX3397 (1  $\mu\text{M}$ , every other day). T-tests was performed.  $n = 4$  lines, \*  $p < 0.05$ . (D) Viability of iMGL following 3-day and 6-day treatments with PLX3397 (1  $\mu\text{M}$ , every other day). Mann-Whitney tests were performed.  $n = 3$  lines, \*\*\*  $p < 0.001$ . (E-F) iMGL were exposed for three hours to pHrodo<sup>TM</sup> Green-labelled myelin debris. Cells were counterstained with Hoechst 33342 and mean green fluorescence intensity (MFI) was measured (a.u. = arbitrary unit). (E) Myelin uptake by iMGL three day after siCON or siCSF1R transfection. (F) Myelin uptake by iMGL following a 3-day treatment with PLX3397 (1  $\mu\text{M}$ , every other day). A t-test was performed.  $n = 3$  lines. (G-H) Cytokine concentrations measured in cell supernatants following a 24-hour treatment with Pam<sub>3</sub>CSK<sub>4</sub> (100 ng/mL). Two-way ANOVA were performed, followed by Tukey's post hoc test. ns = non-significant. (G) Cells were used three days after transfection with siCON or siCSF1R;  $n = 3$  lines. (H) Cells were treated for three days with PLX3397 (1  $\mu\text{M}$ , every other day);  $n = 4$  lines.

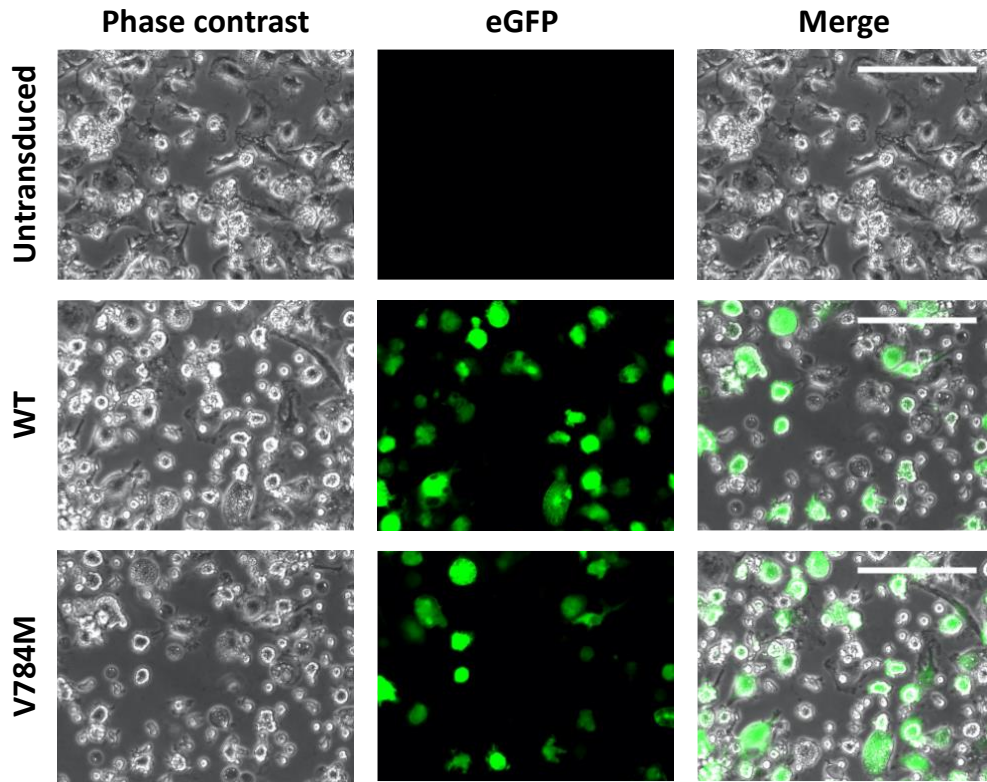


**Figure S27. Phase contrast and green fluorescence images of transduced ALSP-CSF1R iMGL.** eGFP and either WT or V784M CSF1R were stably co-expressed in ALSP-CSF1R iHPCs using lentiviruses and cells were differentiated into iMGL following the 2.9 protocol. Images were taken on day 28 of microglial differentiation. Scale bar = 150  $\mu$ m.

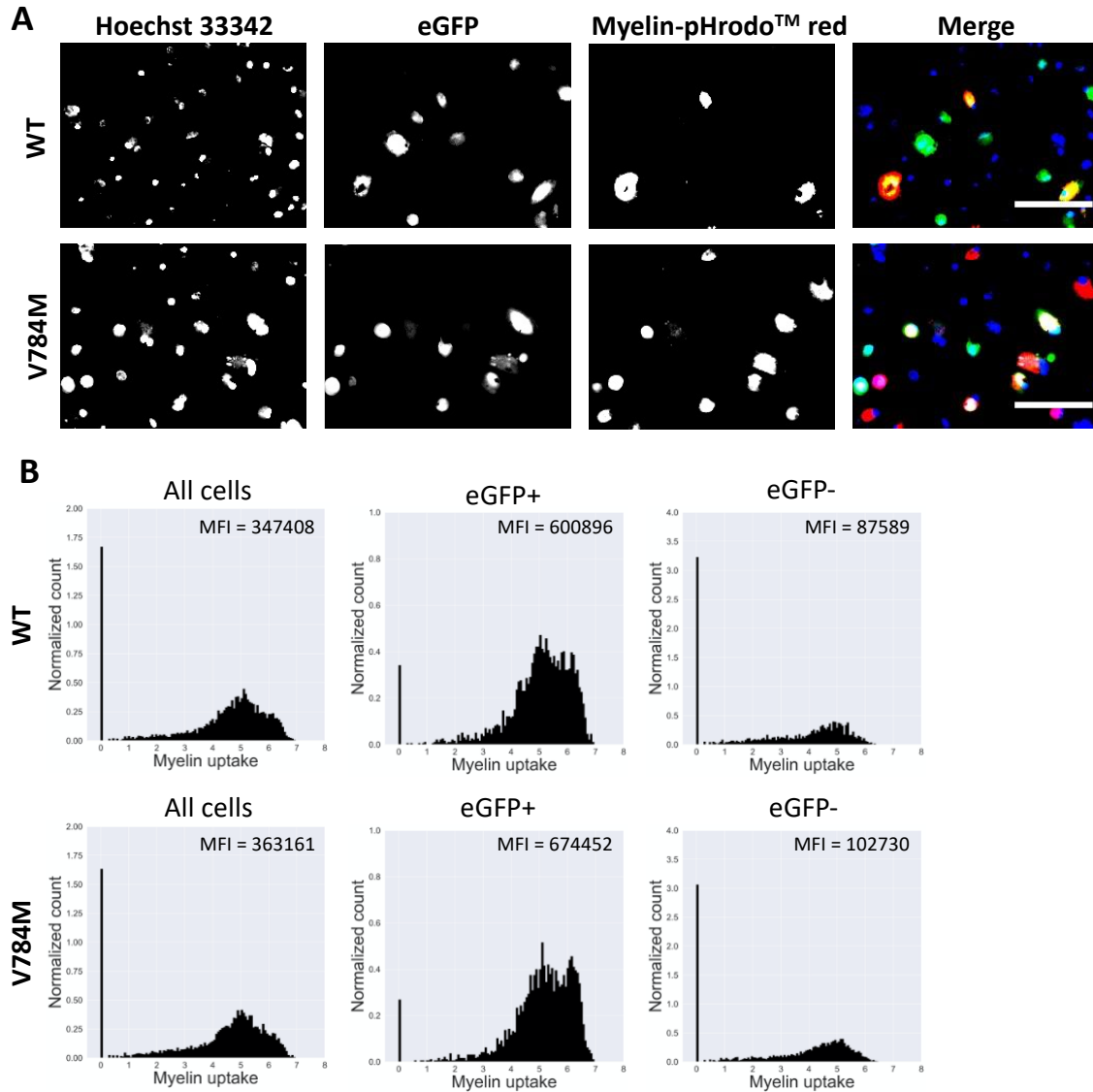


**Figure S28. Effect of lentivirus-induced stable WT and V784M CSF1R expression on myelin uptake by ALSP-CSF1R iMGL.** eGFP and either WT or V784M CSF1R were stably co-expressed in ALSP-CSF1R iHPCs using lentiviruses and cells were differentiated into iMGL following the 2.9 protocol. iMGL were exposed to myelin pHrodo™ Red for 3 hours and counterstained with Hoechst 33342. (A) Representative fluorescence images. Scale bar = 100  $\mu$ m. (B) Measurement of red fluorescence intensity. MFI = mean fluorescence intensity. n = 1 differentiation batch.